Novel hydrogen storage properties of MoS$_2$ nanotubes

J. Chen*, S.L. Li, Z.L. Tao

Institute of New Energy Material Chemistry, Nankai University, Tianjin 300071, PR China

Received 1 September 2002; accepted 15 November 2002

Abstract

Multi-wall MoS$_2$ nanotubes were prepared using a catalyzed thermal decomposition of $(NH_4)_2MoS_4$. The as synthesized nanotubes were treated with 5 M KOH solution at 50 °C for 1 h. These two nanotubes were characterized by XRD, SEM, TEM/HRTEM, BET, XPS, CV and charge–discharge measurements. The results show that MoS$_2$ nanotubes can store relatively large amounts of hydrogen by gaseous and electrochemical storage. The adsorption–desorption reactions are highly reversible at the temperature of 25 °C, implying that these nanotubes are promising materials for hydrogen storage.
© 2003 Elsevier B.V. All rights reserved.

Keywords: MoS$_2$; Nanotube; Hydrogen storage; Characterization

1. Introduction

Effective reversible hydrogen storage plays an important role in practical use of hydrogen energy. One method, which has been rigorously studied, involves the utilization of metals, alloys, complexes, and 'controversial' advanced carbon materials [1]. However, among them, no one has been found to meet all the demands required for commercial electric-vehicle applications. Apparently, researchers in the hydrogen storage field must face the challenge on how to look into new material combinations that exhibit high volumetric/gravimetric hydrogen capacity as magnesium-based hydrides and fast kinetics at room temperatures as LaNi$_5$ system.

Graphite is the most stable form of carbon under ambient conditions. Notwithstanding, graphite nanoparticles have been unstable and they close into fullerenes [2] and nanotubes [3]. A large amount of work on the experimental and theoretical studies of hydrogen adsorption has been carried out to measure the storage capacity of carbon nanotubes [4–10]. Using the paradigm of carbon fullerenes, Tenne and co-workers [11,12] reported that nanoparticles of 2-D layered transition-metal dichalcogenides collapse into fullerene-like cages and nanotubes. In our previous paper [13], we described the electro-

chemical hydrogen storage in MoS$_2$ nanotubes with 60% purity. In this study, we report the synthesis of MoS$_2$ nanotubes with 90% purity by a low-temperature catalytic reaction and compare their gaseous and electrochemical hydrogen storage properties.

2. Experimental

Our production for yielding MoS$_2$ nanotubes consists of three steps [14]: the preparation of needle-like $(NH_4)_2MoS_4$ from $(NH_4)_6Mo_{12}O_{39}\cdot12H_2O$, the ball milling of $(NH_4)_2MoS_4$ in H$_2$ atmosphere (0.2 MPa with a Fuji Auto mixer at 800 rpm for 1 h), and the sintering at 400 °C of the as ball-milled sample in a floating hydrogen/thiophene (C_4H_4S) atmosphere (volume ratio of H$_2$:C$_4$H$_4$S=19:1). The gas chromatograph analysis shows that C$_4$H$_4$S is taking the role of catalyst. The gas–solid reaction which occurred during the sintering process is:

$$(NH_4)_2MoS_4 + H_2 \rightarrow MoS_2 + 2NH_3 + 2H_2S \qquad (1)$$
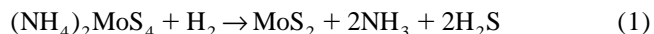
After the reaction was completed, the resulting black solid was treated by 5 M KOH solution at 50 °C for 1 h. Then, the solid was filtered, washed with deionized water several times, and finally dried in a vacuum at 80 °C for 1 h.

The untreated and treated samples were analyzed by XRD (Rigaku INT-2000, 40 kV/150 mA), SEM (Jeol

*Corresponding author.
E-mail address: chenabc@nankai.edu.cn (J. Chen).

JSM-5600, 15 kV); TEM and HRTEM (Jeol JEM 3000F, 300 kV), XPS (ESCA-3400, Shimadzu Electron), and BET adsorption–desorption (Shimadzu-Micromeritics ASAP-2010).

The gaseous hydrogen adsorption/desorption amounts of polycrystalline MoS_2, untreated and treated MoS_2 nanotubes (about 0.5 g) were determined using an automated Sieverts-type apparatus (Advanced Materials Corporation) in the temperature of 25 °C. The volume in the hydriding/dehydriding process had been carefully calibrated before the actual measurement. Ultra-high purity hydrogen (99.999%) was used. Temperature was controlled to 25 ± 0.1 °C with a circulating water bath around the specimen reactor. Complete isotherms were determined during hydrogen absorption and desorption for the above three samples. However, in brief only the data corresponding to the adsorption process were described.

The MoS_2 electrodes were prepared by the following method. In each case, 0.2 g MoS_2 (untreated or treated nanotubes or polycrystalline powders), 0.1 g nickel powder, and 0.02 g polytetrafluoroethylene were thoroughly mixed and then pressed into a pellet (diameter 1.0 cm) under the pressure of 200 kg cm^{-2}, which was sandwiched in nickel foam and attached to a nickel tape for connection.

The MoS_2 electrode was tested in an open cell by using a sintered $Ni(OH)_2/NiOOH$ counter electrode and a Hg/HgO reference electrode in 5 M KOH solution at 25 °C. Discharge capacities were measured at various current densities by using an automatic galvanostatic charge–discharge unit interfaced with a computer. The electrochemical performance was investigated by means of Solartron SI 1260 Potentionstat Analyzer with 1287 Interface and an Arbin charge–discharge unit. The discharge capacity of the MoS_2 nanotubes in any electrode was based on the amount of the active material (MoS_2) not including the weight of the additives in the electrode.

3. Results and discussion

3.1. Sample characterization

The XRD patterns of the ball milled $(NH_4)_2MoS_4$ before and after thermal reaction are shown in Fig. 1. Comparison of these two diffraction peaks shows that their features look different. In the XRD pattern of Fig. 1a for the sample before thermal reaction, the characteristic peak at $2\theta = 17.2°$ indicates that the phase is orthorhombic structure (ICDD-JCPDS Card No. 48-1662). The peak broadening is owing to the very fine grain size and defects produced during the high-energy ball milling process. However, the diffraction peaks corresponding to $(NH_4)_2MoS_4$ in Fig. 1b disappeared, and new peaks appeared with relatively strong intensities. The XRD

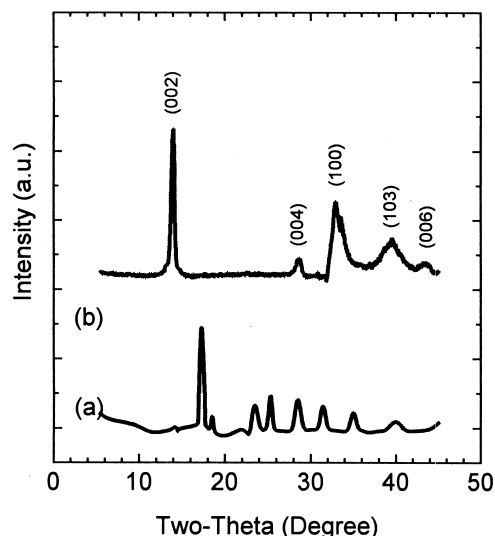Fig. 1. XRD patterns of ball milled $(NH_4)_2MoS_4$ (a) before and (b) after low-temperature catalytic thermal reaction.

pattern in Fig. 1b coincides well with that of polycrystalline MoS_2 (ICDD-JCPDS Card No. 39-1492).

The SEM observations show that polycrystalline MoS_2 powder consists of micrometer particles (Fig. 2a), but the samples without and with KOH treatment are characterized by a large quantity of wirelike nanostructures with typical lengths of several hundreds of nanometers (Fig. 2b and c).

Fig. 3a is a typical TEM image of the sample without KOH treatment, showing that the product consists of many nanotubes. Fig. 3b shows the HRTEM image, which demonstrates that the nanotube tip is completely open. The outer diameter of a typical hollow tube is ~25 nm, while the inner diameter is ~10 nm. The average distance between each two neighbouring fringes ($c/2$) is 0.63 nm, which corresponds to the interlayer (002) d-spacing of the $2H-MoS_2$ lattice. It is noted that for the sample with KOH treatment, more defects were detected around the nanotube walls (Fig. 3c). Based on the SEM, TEM, and HRTEM analyses, we estimated the purity of MoS_2 nanotubes in our products to be more than 90 wt%. The chemical composition of the nanotube was analyzed by energy dispersive X-ray spectroscopy (EDXS), giving an atomic Mo/S ratio of 1.0:2.0. The XPS analysis shows that the chemical valence of molybdenum in the nanotubes is +4 owing to the fact that a binding energy of 228.9 eV, which can be assigned to $Mo3d_{5/2}$ in MoS_2, is detected. Therefore, the as synthesized sample is MoS_2 nanotubes.

BET measurements by the nitrogen gas adsorption/desorption method show that the specific surface area (SSA) of polycrystalline MoS_2 is only 3.6 m^2 g^{-1}, whereas the SSA values of untreated and treated MoS_2 nanotubes are 22 and 28 m^2 g^{-1}, respectively. These results suggest that the SSA of MoS_2 nanotubes is much
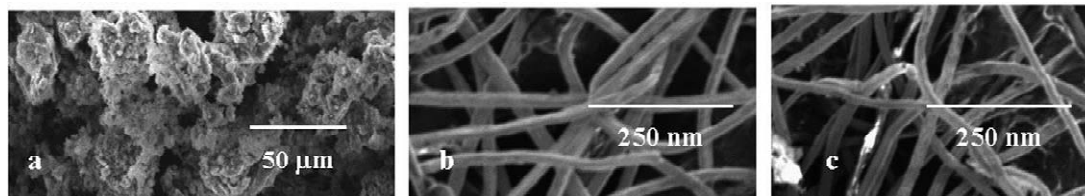
Fig. 2. SEM images of MoS$_2$: (a) polycrystalline, (b) nanotubes without KOH treatment, and (c) nanotubes with KOH treatment.

larger than that of the polycrystalline material and that the KOH treatment is effective in increasing the SSA, possibly owing to the production of defects.

3.2. Gaseous storage

Fig. 4 shows that the hydrogen storage capacities for the above three samples from the highest capacity to the lowest are in the order of MoS$_2$ nanotubes with KOH treatment > MoS$_2$ nanotubes without KOH treatment > polycrystalline MoS$_2$. This order illustrates that higher specific surface areas are responsible for the improved hydrogen adsorption behavior. When adsorption equilibrium was achieved, the hydrogen in the system was vented.

The container with the powders was then weighed. There exists little weight increase (about 0.15%), revealing that most hydrogen could be desorbed at 25 °C, but some still remained.

3.3. Electrochemical storage

We previously investigated reversible hydrogen adsorption/desorption through cyclic voltammetric analysis [13]. The results are briefly described. First, a cathodic peak appeared with the peak position at −0.955 V vs. Hg/HgO, attributed to hydrogen reduction on the Ni/MoS$_2$ site, whereas an anodic peak was observed at −0.645 V vs. Hg/HgO, being assigned to the hydrogen oxidation. Second, the values of peak currents of hydrogen reduction/oxidation for MoS$_2$ nanotubes were much higher than that of the polycrystalline MoS$_2$ electrode. Third, the peak similarity between the hydrogen reduction and oxidation indicates that the electrochemical hydrogen adsorption/desorption proceeds reversibly. Fourth, the peak currents for hydrogen reduction and oxidation are quite sensitive to SSA, and they increase as the SSA increases. Consequently, it appears that the electrochemical charge–dis-
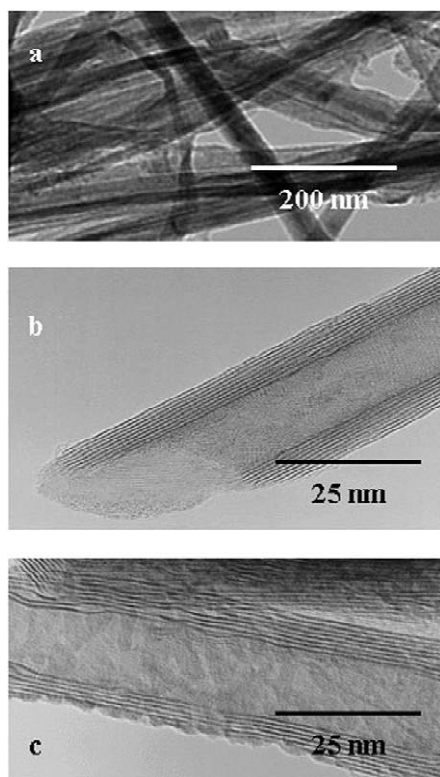

Fig. 3. (a) TEM and (b) HRTEM images of MoS$_2$ nanotubes without KOH treatment, and (c) HRTEM image of KOH-treated MoS$_2$ nanotubes.
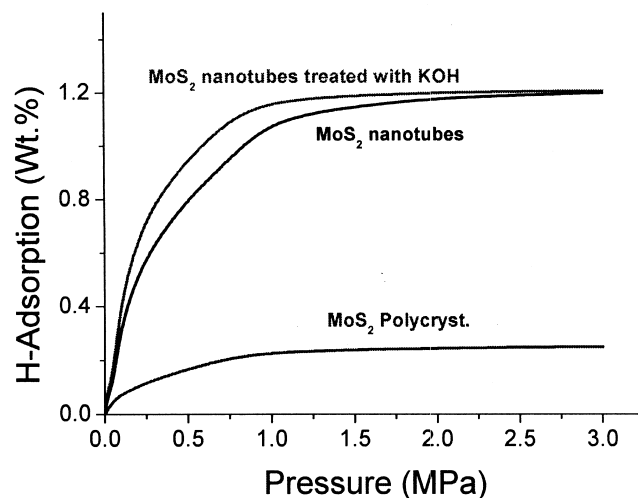

Fig. 4. The hydrogen adsorption amount vs. pressure of polycrystalline MoS$_2$, and nanotubes without and with KOH treatment at 25 °C.
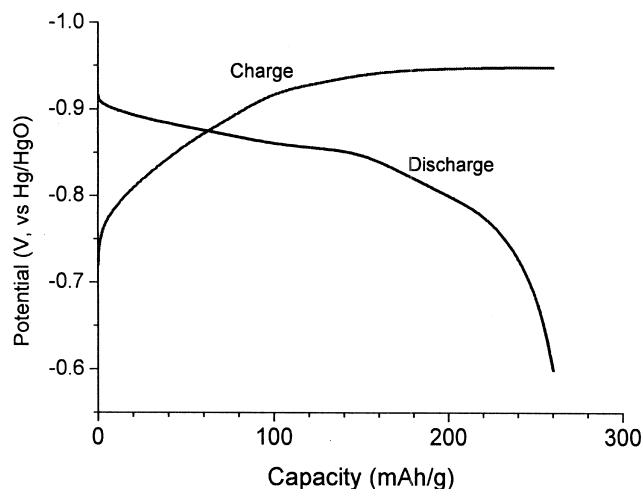
Fig. 5. The electrode charge–discharge curves of MoS_2 nanotubes (with KOH treatment) at 25 °C.

Fig. 7. Cycle life of the MoS_2 nanotube (with KOH treatment) electrode.

charge mechanism occurring in MoS_2 nanotubes is somewhere in between the carbon nanotubes (physical process) and metal hydride electrodes (chemical process), and consists of the charge transfer reaction and diffusion step.

Fig. 5 shows the charge–discharge curves of MoS_2 nanotube (with KOH treatment) electrode at the 5th cycle and the discharge current density of 50 mA g^{-1}. The absolute value of the electrode potential increased gradually during the charging process, while it decreased in the discharging step. A maximum discharge capacity of 262 mAh g^{-1}, corresponding to about 1.0 wt% hydrogen, was achieved. This capacity is about 83% of that obtained in the gaseous storage.

Fig. 6 shows the discharge capacity vs. discharge current densities for the MoS_2 nanotube (with KOH treatment) electrode. When the discharge current density was 50
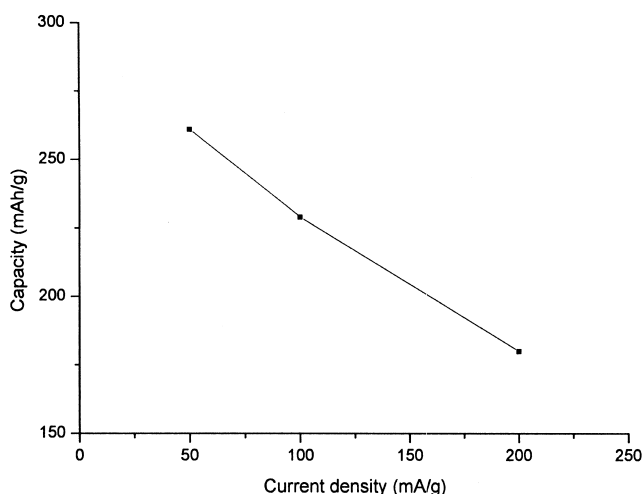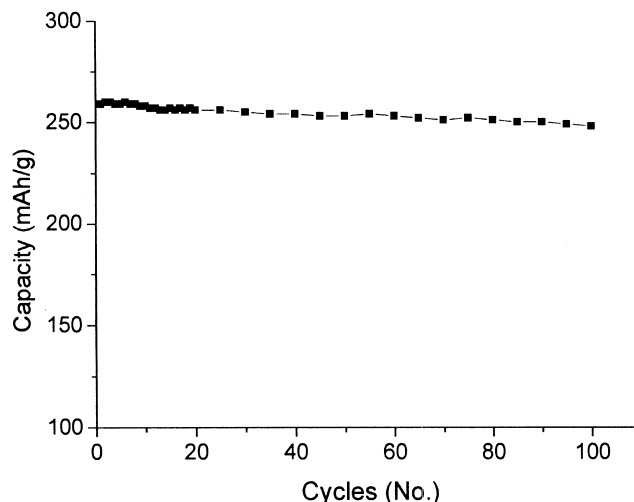
mA g^{-1}, the electrode discharge capacity was 262 mAh g^{-1}. As a comparison, at the discharge current density of 200 mA g^{-1}, the electrode discharge capacity was 182 mAh g^{-1}, which showed a decrease of about 30%.

Fig. 7 shows the change of discharge capacity for the MoS_2 nanotube (with KOH treatment) electrode during 100 cycles. After the test to 100 consecutive cycles of charging and discharging (100% DOD at 100 mA g^{-1}), the capacity of the nanotube electrode decreased by only about 5%, showing a stable electrode property.

4. Conclusions

We have demonstrated that MoS_2 nanotubes, which were synthesized by heating ball-milled $(NH_4)_2MoS_4$ in hydrogen/thiophene atmosphere at a relatively low temperature of 400 °C, can reversibly store hydrogen by gaseous and electrochemical methods. The KOH treatment of the MoS_2 nanotubes produced larger specific surface area due to the production of more defects. The KOH treated MoS_2 nanotubes showed the highest gaseous storage capacity of 1.2 wt% hydrogen and the highest electrochemical discharge capacity of 262 mAh g^{-1} at 25 °C. Our new results show that the alkaline-treated nanotubes with much higher specific surface areas may be one reason for the improved hydrogen adsorption/desorption behavior. There is an indication that this kind of nanotube (especially the light-transition metal disulfide nanotubes such as TiS_2 nanotubes) may be important for hydrogen storage. The precise mechanism of the hydrogen adsorption/desorption is still not understood and further studies are needed prior to possible applications in effective energy storage and high-energy batteries.

Fig. 6. The discharge capacity vs. discharge current densities for the MoS_2 nanotube (with KOH treatment) electrode.

Acknowledgements

References

[1] L. Schlapbach, A. Züttel, Nature 414 (2001) 353.
[2] H.W. Kroto, J.R. Heath, S.C. O'Brien, R.F. Curl, R.E. Smalley, Nature 318 (1985) 162.
[3] S. Iijima, Nature 354 (1992) 56.
[4] A.C. Dillion, K.M. Jones, T.A. Bekkadahl, C.H. Kiang, D.S. Bethune, M.J. Heben, Nature 386 (1997) 377.
[5] A.C. Dillion, M.J. Heben, Appl. Phys. A 72 (2001) 133.
[6] V. Meregalli, M. Parrinello, Appl. Phys. A 72 (2001) 143.
[7] R.G. Ding, G.Q. Lu, Z.F. Yan, M.A. Wilson, J. Nanosci. Nanotechnol. 1 (2001) 7.
[8] C.C. Ahn, Y. Ye, B.V. Ratnakumar, C. Witham, R.C. Bowman Jr., B. Fultz, Appl. Phys. Lett. 73 (1998) 3378.
[9] M. Hirscher, M. Becher, M. Haluska, U. Dettlaff-Weglikowska, A. Quintel, G.S. Duesberg, Y.M. Choi, P. Downes, M. Hulman, S. Roth, I. Stepanek, P. Bernier, Appl. Phys. A 72 (2001) 129.
[10] G.G. Tibbetts, G.P. Meisner, C.H. Olk, Carbon 39 (2002) 2291.
[11] R. Tenne, L. Margulis, M. Genut, G. Hodes, Nature 360 (1992) 444.
[12] L. Margulis, G. Salitra, R. Tenne, Nature 365 (1993) 113.
[13] J. Chen, N. Kuriyama, H.T. Yuan, H.T. Takeshita, T. Sakai, J. Am. Chem. Soc. 123 (2001) 11813.
[14] J. Chen, S.L. Li, Q. Xu, K. Tanaka, Chem. Commun. (2002) 1722.